

Possible origin of nonlinear magnetic anisotropy variation in electric field effect in a double interface system

Daiki Yoshikawa,^{1, a)} Masao Obata,¹ Yusaku Taguchi,¹ Shinya Haraguchi,¹ and Tatsuki Oda^{1, 2}

¹⁾*Graduate School of Natural Science and Technology, Kanazawa University, Kanazawa 920-1192, Japan*

²⁾*Institute of Science and Engineering, Kanazawa University, Kanazawa 920-1192, Japan*

We investigated the effect of an electric field on the interface magnetic anisotropy of a thin MgO/Fe/MgO layer using density functional theory. The perpendicular magnetic anisotropy energy (MAE) increases not only under electron depletion but also under some electron accumulation conditions, showing a strong correlation with the number of electrons on the interface Fe atom. The reverse variation in the MAE under the electric field is ascribed to novel features on the charged interface, such as electron leakage. We discuss the origin of the variation in terms of the electronic structures.

^{a)}Electronic mail: yoshikawa@cphys.s.kanazawa-u.ac.jp

Electric-field- (EF-) driven devices of magnetic materials have been a possible direction for future spin electronic applications for more than ten years¹⁻⁴. Metallic devices with an interface of insulating material have become a promising system. Ultralow energy consumption is strongly expected owing to the nonvolatile nature of magnetism⁵. In magnetic tunnel junctions, duplication of a single junction has been introduced to improve performance⁶. Similarly, in a magnetic device intended to exploit the EF-driven change in the magnetic anisotropy, a proposed double interface structure has shown a large enhancement in the EF-induced effect on the magnetic anisotropy energy (MAE)⁷. In this work, the authors found unusual nonlinear behavior of the EF dependence of the MAE. For both electron depletion and electron accumulation conditions at the interface of the magnetic metallic layer, the MAE changes to favor stability in the magnetic direction perpendicular to the interface plane. The origin of this preference in such a double interface structure is not yet clear. The establishment of nonlinear behavior in the MAE variation may extend the range of applications of EF-driven magnetic devices⁸. A theoretical understanding of the behavior will accelerate development. In this work, we successfully explain this behavior using a realistic model with a double interface, while MAE variation has been investigated theoretically only at single interfaces^{9,10}. We used the MgO/Fe interface, which shows a magnetic anisotropy perpendicular to the interface plane. The effect of B atoms in the magnetic layer⁷ was neglected. This effect has been investigated in the literature^{11,12}.

We used a slab system, vacuum (0.79 nm)/MgO [4 atomic monolayers (ML)]/Fe (3 ML)/MgO (7 ML)/vacuum (0.79 nm), in the computation [Fig. 1(a)]. The atoms are specified by number as Fe(1), Fe(2), ..., O(1), ..., Mg(1), ..., etc., from the left-hand side of the system. The sets of left and right MgO layers are labeled MgO(L) and MgO(R), respectively. There are two MgO/Fe interfaces in the model. At each interface, an Fe atom was placed directly next to the O atom because of its stability. This system includes both edges of the magnetic layer, enabling us to investigate the EF effect, which comes from both simultaneously. We carried out a first-principles density functional calculation that uses fully relativistic ultrasoft pseudopotentials and a planewave basis¹³ by using the generalized gradient approximation¹⁴. The MAE was estimated from the total energy difference between the [100] (x -axis) and [001] (z -axis) magnetization directions, that is, $\text{MAE} = E[100] - E[001]$, where [001] specifies the direction on the right-hand side in Fig. 1(a). We used a $32 \times 32 \times 1$ mesh in \mathbf{k} point sampling, and the in-plane lattice constant was fixed at the value for the

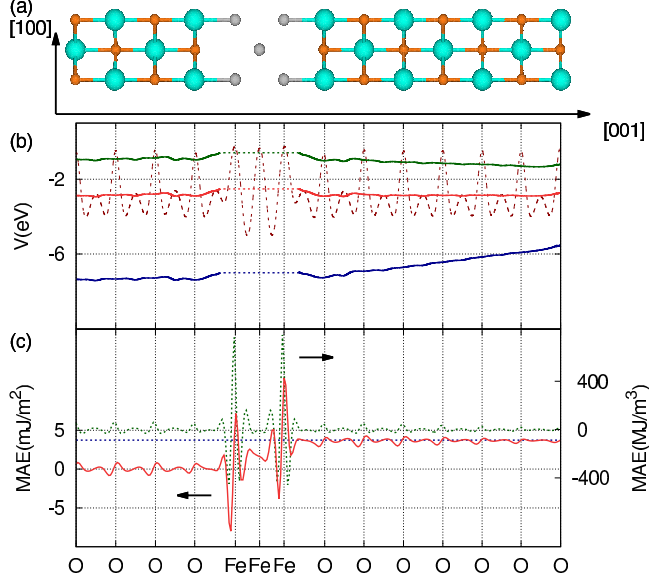


FIG. 1. (a) Atomic configuration of slab, MgO (4 ML)/Fe (3 ML)/MgO (7 ML). (b) Averaged electrostatic potentials for electrons along the z -axis at $E = 0$ (red thin and thick curves), $E = 0.42$ V/nm (blue thick curves), and $E = -0.26$ V/nm (green thick curves). (c) MAE distribution averaged over the xy -plane (green dotted curve) and integrated along the z -axis (red thick curve). Blue dotted line specifies the MAE (3.73 mJ/m²) at $E = -0.16$ V/nm.

MgO layer extracted from the bulk ($a = 0.298$ nm). We induced structural relaxation at zero EF while maintaining both the in-plane lattice constant and the atomic coordinates of Mg(1) and O(1) in a plane perpendicular to [001]. To apply the EF, we placed an effective screened medium (ESM)¹⁵ on the right-hand edge of the slab system (adjacent to the vacuum). This medium acts like an ideal metal, accumulating charge on its surface when the slab system becomes charged. Therefore, by introducing a change in the number of electrons (NOE) in the slab, an EF is imposed on the slab from the right, causing an EF to appear on the magnetic layer in the MgO(R) layer. Consequently, we could investigate the effects of the EF on the magnetic metallic layer sandwiched with MgO. This situation is thought to be similar to that in experimental work⁷, in which most of the applied voltage falls across the thicker MgO layer corresponding to MgO(R). The external EF E_{ext} can be estimated from the gradient of the electrostatic potential at the front of the ESM in the vacuum layer. The details of the EF application are given in a previous work¹⁶. The MAE will be discussed with respect to the realistic EF E , which is obtained from $E = E_{\text{ext}}/\varepsilon_r$, where $\varepsilon_r (= 9.8)$ is

the relative dielectric constant for MgO. EFs of 0.42, 0.21, 0.0, -0.10 , -0.16 , -0.21 , and -0.26 V/nm were obtained, with electron depletions or accumulations in the slab of -0.02 , -0.01 , 0.0, 0.005, 0.0075, 0.01, and 0.0125, respectively. We calculated the MAE density by analyzing the real-space distribution of the MAE^{16,17}.

At the interfaces, the distances between the Fe and O atoms were estimated to be 2.22 Å. This value is consistent with experimental and theoretical values determined in these interface configurations^{10,18}. The Mg atoms were relaxed in the direction of the Fe layer by a small displacement, such as 5 pm,¹⁰ from the O layer. This means that there existed an electric polarization directed in the perpendicular (z -axis) direction. The Mg displacement is a consequence of the electron transfer caused by orbital hybridization between Fe $3d(3z^2 - r^2)$ and O $2p(z)$, which is partially reduced by the displacement of electron densities on the Mg atom. As a result of the electronic structures and electric polarizations at the MgO/Fe interface, the electrons with energy around the Fermi level did not inhabit firmly stable states on Fe(1) and Fe(3). From the analyses in our calculation, the electron potential at the interface rose at the Fe and decreased at the MgO, as shown in Fig. 1(b). In this figure, the electrostatic potential for $E = 0$ averaged within the plane normal to $[001]$ is presented as a broken curve, in addition to the further averaged potentials (solid green, red, and blue curves) for $E = -0.26$, 0.0, and 0.42 V/nm, which were obtained by averaging data in a period of the layer along $[001]$. The potential shoulder observed at the interface may indicate a novel property of electrons. This potential weakens the ability to hold electrons on the Fe; that is, the number of electrons on the Fe becomes sensitive to the external EF. In Fig. 1(c), the real-space variation in the MAE and the integrated distribution along the z -axis are presented. These curves help us to understand that the MgO/Fe/MgO magnetic layer/interface produces perpendicular magnetic anisotropy (positive MAE). Unfortunately, because of the smallness of the MAE variation, these curves could not be used to identify the EF effect.

The MAEs with respect to the EF are presented and compared with experimental data⁷ in Fig. 2. To check an unambiguity on the number of MgO layers, we also estimated the MAEs in a similar system, MgO (5 ML)/Fe (3 ML)/MgO (6 ML). The EF-induced variation in the MAE did not change except for small uniform increases by about 0.003 mJ/m². The perpendicular magnetic anisotropies were obtained and were consistent with previous theoretical calculations and experimental observations^{19,20}. The depletion of electrons on the

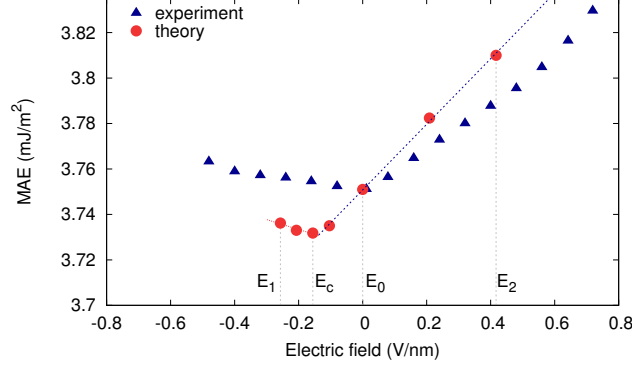


FIG. 2. EF variation of MAE (red circles) compared with the experimental data (blue triangles), which are adjusted to the MAE value at zero EF.

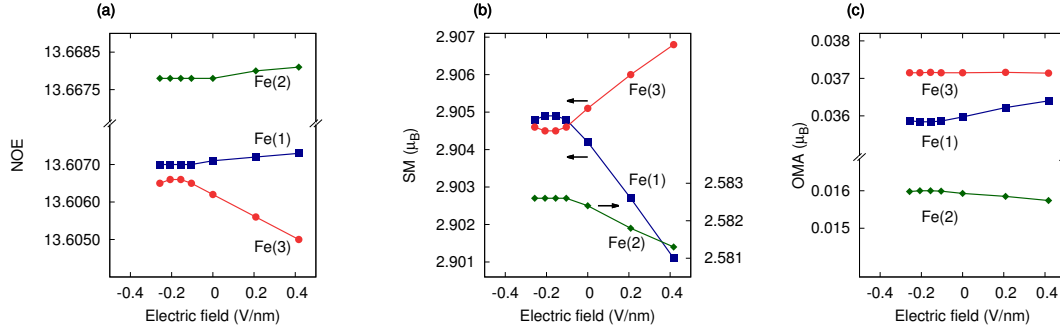


FIG. 3. EF variations in (a) NOE on Fe (1) (blue circles), Fe (2) (green diamonds), and Fe (3) (red squares), (b) atomic SM, and (c) OMA.

interface, which corresponds to a positive EF, increased the MAE at a rate of 144 fJ/Vm. This rate is in good agreement with experimental data^{21,22}, theoretical estimations^{9,19}, and, in particular, the experiment on the double interface (108 fJ/Vm)⁷. The electron accumulation caused the MAE to decrease at the same rate as under a positive EF until $EF = E_c$ and subsequently reversed the variation in the MAE. This reverse corresponded well to an experimental observation whose origin was not clarified⁷. The variation rate at $E < E_c$ was estimated to be -43 fJ/Vm, which is comparable to the experimental value (-24 fJ/Vm)⁷.

To approach the origin of the effect of the EF on the MAE variation, the NOE, spin magnetic moment (SM), and orbital magnetic moment anisotropy (OMA)²³ were investigated.

The atomic quantities are presented in Fig. 3. The MAE has been discussed in terms of the variation in the NOE²⁴. As shown in Fig. 3(a), the variation in the NOE on Fe(3) was apparently correlated with the MAE variation shown in Fig. 2. Further, most of the variation in the MAE is described by a rate of -47 (-40) mJ/m² per NOE on Fe(3) at EFs larger (smaller) than E_c . There is an interesting feature in the variation in the NOE. When the NOE on Fe(3) decreases, that on both Fe(1) and Fe(2) increases, implying electron transfer from Fe(3) to Fe(1) and Fe(2). This contrast in the NOE variations enabled us to recognize the enhancement of electron depletion on Fe(3), highlighting the large effect of the EF on the MAE variation (144 fJ/Vm) at positive EFs. Under a negative EF, the NOE on Fe(3) increased until E_c and then decreased. An analysis of the electron distribution revealed that, at $E < E_c$, the distribution shifted toward the surface of MgO(R) in our model. This implies that, in the experimental system, electrons move into the insulating MgO(R) layer at negative EFs [see the negative slope of the electrostatic potential in Fig. 1(b)]. Note that such a density shift in our model never implies electrons occupying the state in the vacuum region.

The Fe atom at the interface has a large magnetic moment ($\sim 3 \mu_B$), as shown in Fig. 3(b). This indicates a large exchange splitting (~ 3 eV) in the electronic structure. Because of this structure, a decrease (an increase) in the NOE usually corresponds to an increase (a decrease) in the SM. However, in Fig. 3(b), the EF-induced variation in the SM on Fe atoms may be enhanced by the spin flip in Fe. This is because the slope of the variation in the SM becomes steeper than that expected from the variation in the NOE. According to Bruno's relation²⁵, the OMA may reflect the behavior of the MAE. In Fig. 3(c), the variations imply an EF dependence of the MAE. The sum of the OMAs over Fe atoms (not shown) increased (decreased) under EFs in the range of $E > E_c$ ($E < E_c$). However, assuming an atomic spin-orbit coupling, the variation rates of the MAE were much lower than those from the total energy computation and experiment (-0.2 and 16 fJ/Vm for $E < E_c$ and $E > E_c$, respectively).

The projected densities of states (PDOSs) on Fe(3) around the Fermi energy E_F are shown for $E = E_c$ in Fig. 4. The corresponding PDOSs on Fe(1) were very similar to those on Fe(3). The PDOSs on Fe(2) did not make any large contribution around E_F . Interestingly, the orbitals of $d(xz) + d(yz)$ and $d(xy)$ had peaks 0.2 eV above E_F at $E = E_c$. These atomic orbitals extended in the angular directions along which there is no covalent bond to

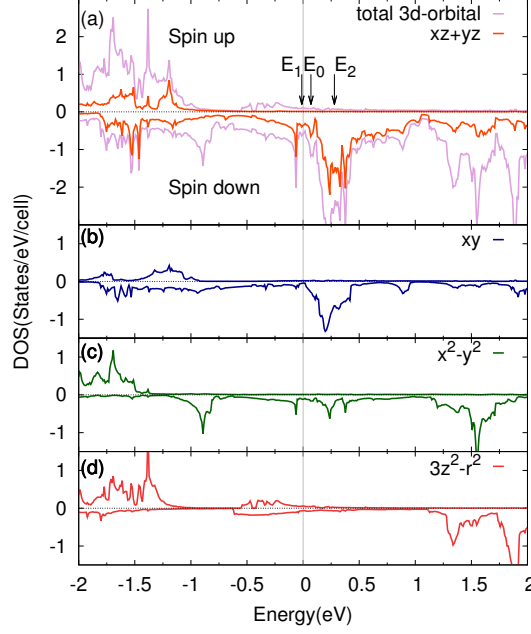


FIG. 4. PDOS at E_c on the 3d orbitals of Fe (3). (a) Total 3d orbital and $d(xz) + d(yz)$, (b) $d(xy)$, (c) $d(x^2 - y^2)$, (d) $d(3z^2 - r^2)$. Vertical line and arrows indicate the location of the Fermi level at $E = E_c$, $E_0(= 0)$, $E_1(= -0.26 \text{ V/nm})$, and $E_2(= 0.42 \text{ V/nm})$. Note that the EF-induced changes in the structure of the PDOS are negligible.

the interface. They were localized at both Fe(1) and Fe(3) and did not exist on Fe(2). The peaks in the PDOSs come from two-dimensional van Hove singularities at the flat bands (not shown) in the momentum space (first Brillouin zone). Such localized and dispersionless electronic states may play a role in capturing electrons when they are occupied. The location of the peaks mentioned above agrees well with those of the interface resonance state (IRS) observed in experiments²⁶. It is also interesting to see that E_F of $E = E_c$ existed at a dip in the total 3d PDOS. This dip may imply the appearance of a reverse point in the EF-induced MAE variation. Note that the E_F value determined in our calculation represents that of the entire system but not that of the metallic layer. Thus, when the EF changed toward positive (negative) values, the location of E_F shifted to a high (low) energy, as indicated in Fig. 4. For example, the location of E_F at $E = E_2$ shifted to around the large peaks as a consequence of the lowered electron potential [see Fig. 1(b)] at the magnetic layer. This did not indicate that the IRS was occupied by the redistributed electron. If it is possible to

define an effective E_F for the magnetic layer, it should be located near E_F for $E = E_0$.

Although the present theoretical model has three magnetic MLs, the increase in Fe layers induces the in-plane component of the magnetic anisotropy due to the magnetic dipole-dipole interaction in the two-dimensional alignment of the magnetic moments²⁷. Taking into account such magnetic anisotropy, which is insensitive to the EF, the total MAE can be reduced to a small positive energy (~ 0.6 mJ/m², assuming an Fe layer 1.5 nm thick)²⁷,) such as the observed MAE (0.31 mJ/m²)⁷.

In our model system, the negative slope of the MAE variation at a finite negative EF is understood to represent electron leakage from the interface to the MgO(R) layer, particularly to the surface adjacent to the vacuum layer. In the real system⁷, the existence of charging spots (places where electrons are trapped) in the MgO(R) layer may be needed to explain the observed negative bias voltage. There could be an impurity site or a defect site in such systems. A probable site of origin is the B or O element. The existence of charging spots is consistent with the fact that the variation in the NOE is reduced on the interface at EFs below E_c . The number of negative charges at the charging spots increases as the external EF decreases, reducing the effective EF imposed on the Fe/MgO(R) interface. In addition, another candidate for charging spots is an IRS at another MgO/Fe interface. This IRS should be assumed not to contribute to electron conduction along the perpendicular direction. In the previous experiment⁷, there is an Fe-alloy/MgO/Fe junction, in which the IRS at MgO/Fe²⁸ may act as a charging spot when negative voltages are applied, supposing that the IRS forms a set of localized states (nonconducting states).

As shown in Fig. 2, the EF at which the inverse variation occurs is shifted from zero EF in the theoretical approach, in contrast to the experiment. This feature may be attributed to the difference between the model and real systems, in particular the thickness of the magnetic layer sandwiched by MgO and the magnetic material itself. This is inferred from the fact that the reverse point of E_c should depend on the details of the electronic states around E_F . If the magnetic layer becomes thicker, that is, the number of electrons increases (as for $E < 0$), the substantial E_F for the entire system may shift from E_0 toward E_c . The lack of theoretical data for $E < E_1$ is related to an inaccurate energy position of the O 2p level (less binding) at the interfaces, which is improved by an advanced electronic structure calculation approach, such as the quasiparticle selfconsistent GW approximation²⁹. These problems might be solved in future studies for the development of EF-driven magnetic

devices.

In summary, we studied the effect of an EF on the interface magnetic anisotropy in the double interface system MgO(L)/ Fe/MgO(R). A first-principles electronic structure calculation indicated that nonlinear behavior of the MAE was the intrinsic feature of such a magnetic layer with an interface. The variations of the MAE with the EF are in good agreement with the experimental values both for $E < E_c$ and $E > E_c$. Our theoretical approach revealed that, under electron depletion, the decrease in the NOE at the Fe in Fe/MgO(R) was enhanced by the existence of the MgO(L)/Fe interface, whereas under electron accumulation, an electron leak occurred on the Fe in Fe/MgO(R), leading to an increase in the MAE. The electronic structures indicate that such a leak is also intrinsic in the magnetic layer with the interface. The theoretical base obtained here greatly encourages experimental research on such nonlinear behavior to develop new EF-driven devices that use the MAE.

Acknowledgements

The authors thank T. Nozaki and M. Otani for stimulating discussions. The computation in this work was performed using the facilities of the Supercomputer Center, Institute for Solid State Physics, University of Tokyo. This work was supported in part by Grants-in-Aid for Scientific Research from JSPS/MEXT (Grant Nos. 22104012 and 23510120) and the Computational Materials Science Initiative (CMSI), Japan.

REFERENCES

- ¹H. Ohno: Nat. Mater. **9** (2010) 952.
- ²H. Ohno, D. Chiba, F. Matsukura, T. Omiya, E. Abe, T. Dietl, Y. Ohno, and K. Ohtani: Nature **408** (2000) 944.
- ³M. Weisheit, S. Fähler, A. Marty, Y. Souche, C. Poinsignon, and D. Givord: Science **315** (2007) 349.
- ⁴T. Maruyama, Y. Shiotani, T. Nozaki, K. Ohta, N. Toda, M. Mizuguchi, A. A. Tulapurkar, T. Shinjo, M. Shiraishi, S. Mizukami, Y. Ando, and Y. Suzuki: Nat. Nanotechnol. **4** (2009) 158.
- ⁵Y. Shiotani, T. Nozaki, F. Bonell, S. Murakami, T. Shinjo, and Y. Suzuki: Nat. Mater. **11** (2012) 39.
- ⁶H. Naganuma, L. Jiang, M. Oogane, and Y. Ando: Appl. Phys. Express **4** (2011) 019201.

- ⁷T. Nozaki, K. Yakushiji, S. Tamaru, M. Sekine, R. Matsumoto, M. Konoto, H. Kubota, A. Fukushima, and S. Yuasa: Appl. Phys. Express **6** (2013) 073005.
- ⁸Y. Suzuki, H. Kubota, A. Tulapurkar, and T. Nozaki: Phil. Trans. R. Soc. A, **369** (2011) 3658.
- ⁹M. K. Niranjana, C.-G. Duan, S. S. Jaswal, and E. Y. Tsybmal: Appl. Phys. Lett. **96** (2010) 222504.
- ¹⁰K. Nakamura, T. Akiyama, T. Ito, M. Weinert, and A. J. Freeman: Phys. Rev. B **81** (2010) 220409 (R).
- ¹¹K. Hotta, K. Nakamura, T. Akiyama, and T. Ito: J. Korean Phys. Soc. **63** (2013) 762.
- ¹²T. Miyajima, T. Ibusuki, S. Umehara, M. Sato, S. Eguchi, M. Tsukada, and Y. Kataoka: Appl. Phys. Lett. **94** (2009) 122501.
- ¹³T. Oda and A. Hosokawa: Phys. Rev. B **72** (2005) 224428.
- ¹⁴J. P. Perdew, J. A. Chevary, S. H. Vosko, K. A. Jackson, M. R. Pederson, D. J. Singh, and C. Fiolhais: Phys. Rev. B **46** (1992) 6671.
- ¹⁵M. Otani and O. Sugino: Phys. Rev. B **73** (2006) 115407.
- ¹⁶M. Tsujikawa and T. Oda: Phys. Rev. Lett. **102** (2009) 247203.
- ¹⁷M. Tsujikawa, S. Haraguchi, T. Oda, Y. Miura, and M. Shirai: J. Appl. Phys. **109** (2011) 07C107.
- ¹⁸C. Tusche, H. L. Meyerheim, N. Jedrecy, G. Renaud, and J. Kirschner: Phys. Rev. B **74** (2006) 195422.
- ¹⁹R. Shimabukuro, K. Nakamura, T. Akiyama, T. Ito: Physica E **42** (2010) 1014.
- ²⁰S. Ikeda, K. Miura, H. Yamamoto, K. Mizunuma, H. D. Gan, M. Endo, S. Kanai, J. Hayakawa, F. Matsukura, and H. Ohno: Nat. Mater. **9** (2010) 721.
- ²¹T. Nozaki, Y. Shiota, T. Shinjo, and Y. Suzuki: Appl. Phys. Lett. **96** (2010) 022506.
- ²²M. Endo, S. Kanai, S. Ikeda, F. Matsukura, and H. Ohno: Appl. Phys. Lett. **96** (2010) 212503.
- ²³M. Tsujikawa, S. Haraguchi, and T. Oda: J. Appl. Phys. **111** (2012) 083910.
- ²⁴K. Nakamura, R. Shimabukuro, Yuji Fujiwara, and T. Ito: Phys. Rev. Lett. **102** (2009) 187201.
- ²⁵P. Bruno: Phys. Rev. B **39** (1989) 865.
- ²⁶P.-J. Zermatten, G. Gaudin, G. Maris, M. Miron, A. Schuhl, C. Tiusan, F. Greullet, and M. Hehn: Phys. Rev. B **78** (2008) 033301.

- ²⁷L. Szunyogh, B. Újfalussy, and P. Weinberger: Phys. Rev. B **51** (1995) 9552.
- ²⁸W. H. Butler, X.-G. Zhang, and T. C. Schulthess, and J. M. MacLaren: Phys. Rev. B **63** (2001) 054416.
- ²⁹T. Kotani, M. van Schilfgaarde, and S. V. Faleev: Phys. Rev. B **76** (2007) 165106.